Available online at www.sciencedirect.com
SCIENCE DIRECT®
Journal of Power Sources 128 (2004) 270–277
JOURNAL OF POWER SOURCES
www.elsevier.com/locate/jpowsour

Synthesis and electrochemical performance of $LiCr_xMn_{2-x}O_4$ powders by mechanical activation and rotary heating

Gui-Ming Song*, Yu-Jin Wang, Yu Zhou

School of Materials Science and Engineering, P.O. Box 433, Harbin Institute of Technology, Harbin 150001, PR China

Received 1 April 2003; received in revised form 30 September 2003; accepted 6 October 2003

Abstract

Mechanical activation followed by rotary heating has been successfully applied to the synthesis of Cr-doped lithium manganese oxide ($LiMn_2O_4$) powders. The precursor of $LiCr_xMn_{2-x}O_4$ for Li-ion batteries has been synthesized from $LiOH{\cdot}H_2O$, MnO_2, and Cr_2O_3 as starting materials by mechanical activation, which ensured a high level of homogeneity in the chemical composition of the precursor and resulted in a reduction in the synthesis temperature and heating time. Highly crystallized $LiCr_xMn_{2-x}O_4$ ($0.04 \leq x \leq 0.10$) powders were obtained by subsequent rotary heating of the precursor at 550–750 °C for 2 h. Rotary heating enhanced the experimental control in chemical composition, particle size distribution and microstructure of the final products. The optimum mechanical activation condition was determined based on XRD analysis. The synthesized $LiCr_xMn_{2-x}O_4$ powder has a narrow particle size distribution, high discharge capacities and good cyclability. The method of mechanical activation combined with rotary heating should be an excellent technique of decreasing synthesis temperature and shortening heating time, and enhancing the uniformity of particle size of the product.

Keywords: Mechanical activation; Rotary heating; Lithium manganese oxide; Cr-doped spinel; Lithium-ion battery

1. Introduction

In last decade, lithium manganese oxide ($LiMn_2O_4$) has been studied extensively as the cathode material for Li-ion battery from the aspect of low cost of raw material, low toxicity and relatively high energy density [1–3]. However, it is initially difficult to prepare $LiMn_2O_4$ with long charge/discharge cycle life. A very effective way for improving the cycling performance of $LiMn_2O_4$ is to synthesize manganese-substituted $LiM_xMn_{2-x}O_4$ spinel phase by doping with divalent or trivalent ions (M: Al [4,5], Mg [6], Co [7,8], Ni [7], Fe [7,9], Ti [7,9], Zn [10] and Cr [7,9,11–13], etc.).

The traditional synthesis method of $LiMn_2O_4$ is direct solid-solid reaction of oxides or acetates of manganese and either LiOH [14,15], or Li_2CO_3 [16,17] and $LiNO_3$ [18,19] at high temperatures to enhance the diffusion process and obtain a well-ordered structure. Due to this high temperature, there are some disadvantages such as broader particle size distribution, longer reaction time or other unwanted phases. These long heat treatments at high temperatures normally do not provide very effective control of the microstructures since grain growth and overall agglomeration of the particles are always inevitable in these treatments. In addition, the risk of possible volatilization of lithium itself is an inherent problem, which tends to be accentuated due to the long heat treatment cycle. However, solid-state reaction technology is easy and simple, and is one of the most suitable techniques for industrialization.

The disadvantages of the solid-state reaction are mainly the higher synthesis temperature and longer high temperature reaction time, together with the difficulties in the effective controls of chemical composition and microstructures as mentioned above. In recent years, great progress has been achieved in developing new synthesis methods of $LiMn_2O_4$ [20–25]. One of the main approaches is mechanical activation. The work of Kosova et al. on $LiMn_2O_4$ [23–25] showed that mechanical activation decreased significantly the synthesis temperature of $LiMn_2O_4$ and the resulted products exhibited tolerable electrochemical performances. Mechanical activation can produce particle and grain size down to the nanoscale, together with structure defects. Energetic lattice defects, combined with short diffusion distances, are the driving forces of faster solid-state activation and chemical reactions at low temperatures.

* Corresponding author. Present address: Laboratory of Materials Science, Delft University of Technology, Rotterdamseweg 137, 2628 AL Delft, The Netherlands. Tel.: +31-15-2786785; fax: +31-15-2786730.
E-mail address: g.song@tnw.tudelft.nl (G.-M. Song).

0378-7753/$ – see front matter © 2003 Elsevier B.V. All rights reserved.
doi:10.1016/j.jpowsour.2003.10.002

Small initial particle size should facilitate the formation of finely dispersed alloys on lithium insertion and, additionally should ease the diffusion of lithium into the material.

The high temperature furnaces for solid-state synthesized Li-ion cathode materials, at present, are periodical kilns or furnaces. The powders in the equipment are static. Therefore, the temperature field within the powders is often non-uniform during heating or cooling, especially for mass production, which will result in non-uniform chemical composition and non-uniform particle size distribution in a batch of synthesized powders. On the other side, these mechanically activated initial powders easily grow during the following high temperature treatment, and sometime result in abnormal grain growth which causes broader particle size distribution. Furthermore, the traditional solid-state synthesis method increases the difficulty of control of chemical composition and particle size of different batch of products. The particle size, crystalline structure and chemical composition of $LiMn_2O_4$ play critical roles on the electrochemical behavior of the cell [1,26]. So, it is a very important and interesting topic that how to control the particle size distribution, chemical composition and phase structure.

In this paper, mechanical activation and rotary heating are combined to form a new synthesis technique in order to decrease synthesis temperature and reaction time, and also obtain good stoichiometric control of $LiCr_xMn_{2-x}O_4$ spinel with uniform particle size distribution. Here the chromium ion is used as a doping cation to improve the cycling performance of $LiMn_2O_4$. Mechanical milling is used to ensure the uniform mixing of raw materials at nanoscale together with structure defects and short diffusion distance. The resulted precursors are heated using a rotary furnace in order to enhance the uniformity of temperature and particle size of $LiCr_xMn_{2-x}O_4$ product during the high temperature synthesis process.

2. Experimental

Starting materials for preparing $LiCr_xMn_{2-x}O_4$ ($0.04 \leq x \leq 0.10$) were $LiOH{\cdot}H_2O$ (>99%, Chengdu Reagent), Cr_2O_3 (>99%, Beijing Reagent) and electrolytic MnO_2 (>99%, CMD, Xiangtan Manganese Co.) powders. MnO_2, $LiOH{\cdot}H_2O$ and Cr_2O_3 were milled using a planetary ball miller with a weight ratio of stainless steel ball to powder of 10:1, and the milling time ranged from 20 min to 25 h. The rotation speed of the miller was 200 rpm. Then, the milled mixtures were placed into a self-made rotary furnace (see Fig. 1) and heated to 450–750 °C for 2 h. The rotation speed of the elevated temperature furnace tube was 40 rpm.

A Rigaku X-ray diffractometer (Dmax/2400) using Cu Kα radiation and a Philips XL-30 scanning electron microscope were used to characterize microstructures of the milled mixtures and final products. The particle size of the prepared powders was measured with a laser particle size analyzer (Coulter LS 230). The analysis of chemical composition

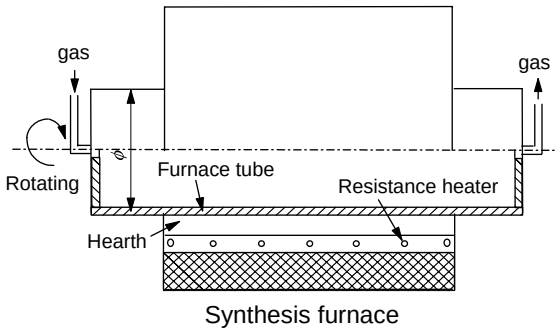

Fig. 1. Schematic of the furnace with a rotary tube.

was carried out with an inductively coupled plasma atomic emission spectrometer (Leeman Profile ICP-AES). The charge/discharge capacity and cyclability were evaluated using a prototype coin cell. The cell comprised a lithium metal electrode and $LiCr_xMn_{2-x}O_4$ electrode that were separated by a polypropylene separator. The $LiCr_xMn_{2-x}O_4$ electrode consisted of 80 wt.% $LiCr_xMn_{2-x}O_4$ powder, 5 wt.% of polytetrafluoroethylene (PTFE) as a binder and 15 wt.% acetylene black. 1.0 M $LiPF_6$ dissolved in ethylene carbonate (EC) and dimethyl carbonate (DMC) (1:1 (v/v)) was used as the electrolyte. The charge and discharge cycling was galvanostatically performed at a current density of 0.3 mA/cm^2 with a cut-off voltage of 3.0–4.3 V (versus Li/Li$^+$) using a potentiostat/galvanostat system (EG&G 273 Instrument).

3. Results and discussion

3.1. Effect of mechanical activation

Fig. 2 shows the XRD patterns of powders milled for various times, herein the Cr content in $LiMn_2O_4$ is designed as $LiCr_{0.06}Mn_{1.94}O_4$. After milling for 20 min, the peaks of MnO_2 become broader, and minor peaks of $LiOH{\cdot}H_2O$ can still be found. As milling time further increases, the intensities of the peaks of MnO_2 and $LiOH{\cdot}H_2O$ decrease and become unidentifiable, and on the same time, the peaks of $LiMn_2O_4$ appear. After 1 h milling, the $LiMn_2O_4$ spinel phase is predominant, which implies that Li–Mn–O spinel takes place when the mechanical activation time is up to 1 h although these peaks of the spinel are broadened suggesting spinel amorphization together with a reduction in crystallite size and a rise in residual mechanical strain. Minor Mn_2O_3 can be found when the milling time is 25 h, which indicates that longer milling time will lead to the formation of other phases.

Lithium hydroxide has a layered structure and good plasticity. Kosova et al. [24,25] thought a “smearing” of LiOH occurred on the surface of MnO_2 particles, and an amorphous layer formed during the initial stage of mechanical activation. The hydroxyl groups were thereby bound by hydrogen bonds to water molecules and locate near paramagnetic manganese ions. Subsequently, electron transferred

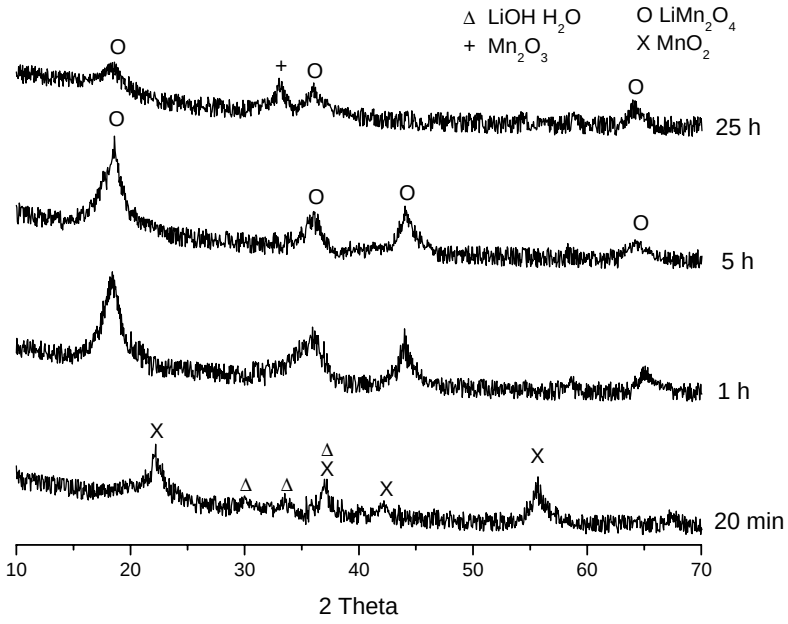

Fig. 2. XRD patterns of mixtures of $LiOH{\cdot}H_2O$, Cr_2O_3 and MnO_2 mechanically activated for various milling times (20 min–25 h), herein the Cr content in $LiMn_2O_4$ is designed as $LiCr_{0.06}Mn_{1.94}O_4$.

from OH groups of $LiOH{\cdot}H_2O$ to the Mn^{4+} ions, partially reducing them to Mn^{3+}. The process is summarized as follows:

$$4LiOH \cdot H_2O + 8MnO_2 = 4LiMn_3 + Mn^{4+}O_4 + 6H_2O + O_2 \quad (1)$$

Further mechanical activation ($\geq$25 h) leads to an amorphization and a decomposition of the Li–Mn–O spinels, with the appearance of new phases mainly identified as Mn_2O_3. Based on the analysis of X-ray patterns of the milled products, we can find a progressive reduction of the manganese oxidation state as well as a modification of the material with increasing milling time. The optimum milling time in this study should be about 5 h. The mechanical energy stored in the milled particles pushes the reaction between $LiOH{\cdot}H_2O$, Cr_2O_3 and MnO_2 to form Cr-doped $LiMn_2O_4$ at low temperature.

Fig. 3 shows XRD patterns of the precursors of $LiCr_{0.06}Mn_{1.94}O_4$ heated at different temperature for 2 h,

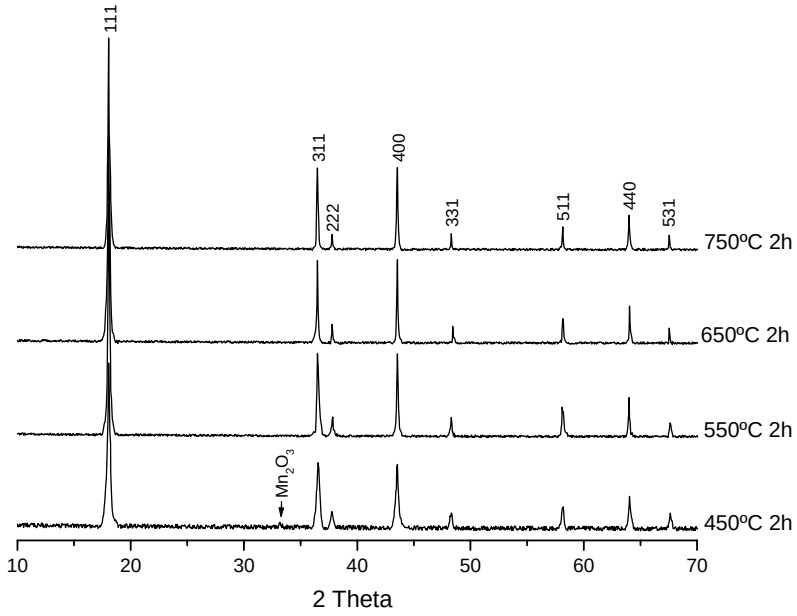

Fig. 3. XRD patterns of mechanically activated precursor heated at various temperatures for 2 h in rotary furnace (450–750 °C), herein the Cr content in $LiMn_2O_4$ is designed as $LiCr_{0.06}Mn_{1.94}O_4$.

herein the precursors were mechanically activated for 5 h. On heating at 450 °C for 2 h, ordered Li–Mn–O spinel is formed, however, minor impure phase mainly identified as Mn_2O_3 exists. With increasing temperature above 450 °C, the peaks of Mn_2O_3 diminish, whereas those of spinel phase increase. At and above 550 °C, well-crystallized cubic spinel with a space group *Fd*-3*m* appears without Mn_2O_3 phase. The lattice constants, which were calculated from XRD data, of crystal cell of the samples heated at 550, 650 and 750 °C are 0.8186, 0.8201 and 0.8230 nm, respectively. There is a slight increase in lattice constant with increasing temperature. The ionic radius of Mn^{4+} (0.0530 nm) is lower than that of Mn^{3+} (0.0645 nm) and Mn^{4+} are more stable at lower temperature [27]. Thereby, the lower lattice parameter indicates the Mn^{4+} content in Li–Mn–O spinel is higher. As we know, the increasing of Mn^{3+} content during the intercalation process brings Jahn–Teller distortion [28,29], which results in a capacity fading of Li–Mn–O spinel. Therefore, lower temperature synthesis is preferable. Compared with the conventional solid-state reaction process, the mechanical activated powders exhibit a lower synthesis temperature and shorter heating time (e.g. 550–750 °C for 2 h), which implies a competitive ability to these currently developing wet-chemical methods (such as sol-gel, Pechini process, etc. [28,30–32]) for low temperature synthesis of Li–Mn–O spinels.

3.2. Effect of rotary heating

Fig. 4a shows a typical micrograph of $LiCr_{0.06}Mn_{1.94}O_4$ powders milled for 5 h followed by heating at 650 °C for 2 h. In order to investigate the effect of rotary heating, the powders synthesized in the same furnace without rotary movement (static heating) is also shown in Fig. 4b. It is significant that the particle size distribution of the products with rotary heating is narrow with an average size of 1.63 μm (see Fig. 5). On the contrary, the particle size of the products without rotary heating is non-uniform, and the average size is 2.47 μm. The statically heated powders are

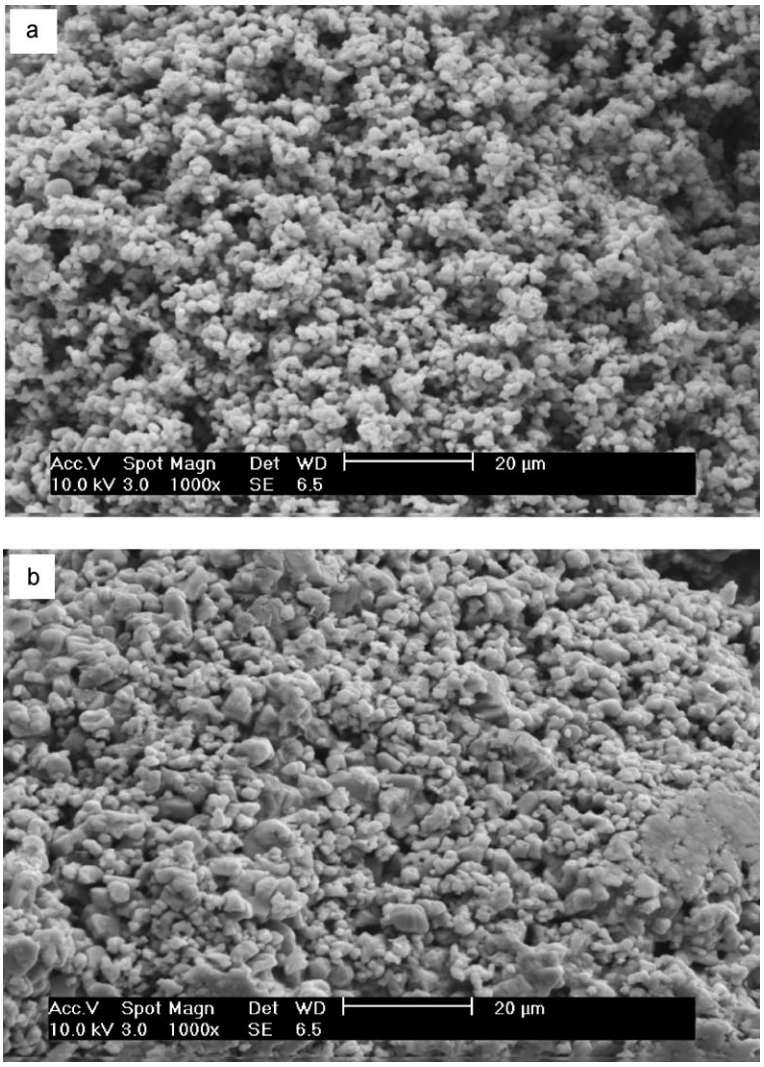

Fig. 4. Micrographs of $LiCr_{0.06}Mn_{1.94}O_4$ powders synthesized at 650 °C for 2 h. (a) The powders synthesized by rotary heating show uniform particle size distribution; (b) the statically calcined powders show uneven particle size distribution.

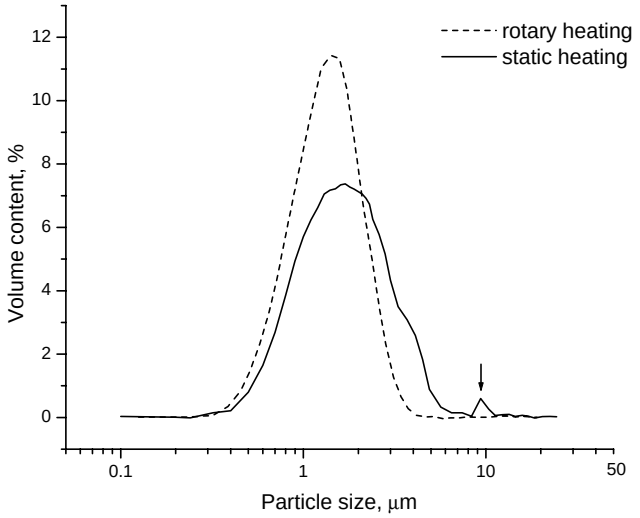

Fig. 5. Particle size distribution of $LiCr_{0.06}Mn_{1.94}O_4$ powders synthesized at 650 °C for 2 h. The powders synthesized by rotary heating show uniform particle size distribution. Inversely, the statically synthesized powders show uneven particle size distribution and abnormal grain growth.

bigger than the powders prepared by rotary heating. There are two peaks in the particle size distribution curve of the statically heated powders, which implies that abnormal grain (or particle) growth took place (marked by arrow in Fig. 5) in the powders during static heating. In Fig. 4b, some big particles (their sizes are over 5 μm) can be found. The SEM observation on the particle size distribution is consistent with the measured results by the particle size analyzer.

During the high temperature synthesis process, there are often several parallel, as well as competing, reactions and processes that are taking place. Therefore, it is desirable to have as high a thermal conductivity as possible to maximize this heat transfer in order for heat to be transferred at as high a rate as possible, which ensures a uniform temperature field in the piled powders (especially for mass production) and is commensurate with the prevention of other undesirable reactions and processes. Chemical reactions, element diffusions and grain growth within the mechanically activated precursor with higher activation energy easily take place at high temperature. If the temperature field is not enough uniform during the whole high temperature period, the reaction and grain growth in higher temperature zone should easily take place at a higher rate. When powders are static in the furnace, some fine particles will sinter together to form coarse particles, and coarser particles will grow bigger and bigger with the time. Thereby, abnormal grain (or particle) growth will take place. Inversely, when the precursor powders are introduced into the rotating furnace, the powders are agitated and exposed to the reaction temperature by means of the rotation of the tube and the associated stirring or tumbling action of the materials. Through this method, the temperatures of these powders are all made be uniform. Therefore, the grain (or particle) growth rate within all the powders almost should be same. Additionally, the stirring, tumbling action

Table 1
Chemical composition and particle size of the samples of three batches of $LiCr_{0.06}Mn_{1.94}O_4$ powders synthesized at 650 °C for 2 h

	Batch 1	Batch 2	Batch 3
Li (wt.%)	3.86	3.82	3.83
Cr (wt.%)	1.62	1.63	1.87
Mn (wt.%)	59.1	58.8	58.6
Li/Cr/Mn (atom ratio)	1/0.056/1.936	1/0.057/1.942	1/0.065/1.931
Average diameter (μm)	1.63	1.56	1.60

associated with interactive grinding among the powders, in a way, fines the powders and prevent abnormal particle growth. That is why the products prepared by rotary heating have smaller particle size and much narrow particle size distribution compared with the powders prepared by static heating.

Three batches of $LiCr_{0.06}Mn_{1.94}O_4$ were synthesized at 650 °C for 2 h using the same technique. The elemental compositions of Li, Cr and Mn and the average particle size of these powders are given in Table 1. The atom ratio of Li/Cr/Mn is in the range of 1/0.056–0.065/1.931–1.942, which is approximately 1/0.06/1.94. The average size of the three batches varies in the range of 1.58–1.63 μm. The above results imply that the chemical composition and average particle size of different batches of products are stable and almost invariant, which indicates a good quality control and quality stability of $LiCr_{0.06}Mn_{1.94}O_4$ products. Here, we also detected the Fe content in the products with ICP-AES method. Iron was brought into the precursor during milling by stainless steel balls and stainless steel jar. However, the Fe content is low, waving at 0.27 wt.% when the milling time is 5 h. Fe impurity was not detected by XRD patterns due to its low content. According to the results of Kumar et al. [7] and Amine et al. [9], Fe can been used as doping ion of $LiMn_2O_4$ spinel, and Fe doped $LiMn_2O_4$ has a good cyclability. Therefore, a very small amount of Fe existing in $LiCr_xMn_{2-x}O_4$ should have no unbeneficial influence to the electrochemical performance of the final products.

The good uniformity of particle size is caused by two reasons: (1) mechanical activation resulted in an uniform particle size; (2) the milled precursors and final products were in a stirring and tumbling state during high temperature synthesizing, which made the temperature and particle size of the materials uniform.

The average size of the $LiCr_{0.06}Mn_{1.94}O_4$ powders synthesized at 450–750 °C for 2 h was shown in Fig. 6, where the precursors were mechanically activated for 5 h. The average size of these powders increased fast from 0.44 μm for 450 °C to 3.87 μm for 750 °C, which demonstrates that the synthesis temperature has a great influence on the average size of the final powders, and also shows that the activated precursors easily grow at high temperature. Therefore, the control of synthesis temperature and calcining time becomes

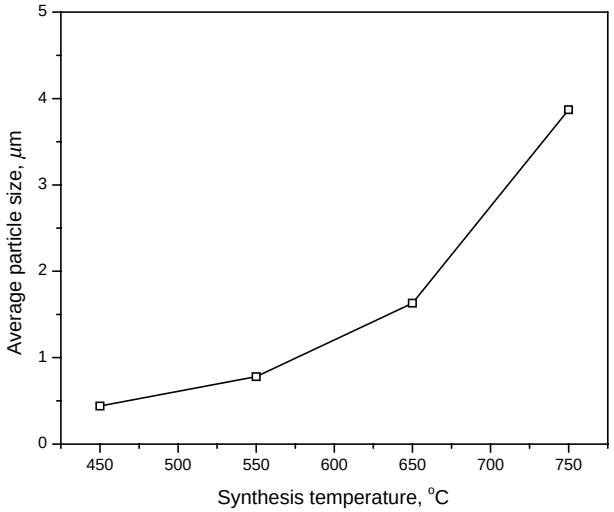

Fig. 6. Average particle size of $LiCr_{0.06}Mn_{1.94}O_4$ powders synthesized at various temperatures for 2 h.

very important for the activated precursors. Rotary heating is an effective method to achieve a uniform temperature field within the powders so as to control physical characterization of the final products.

Fig. 7 gives the influence of doped Cr^{3+} ion content in $LiCr_xMn_{2-x}O$ spinel on the average size of the final products synthesized at 650 °C for 2 h, herein all the precursors were milled for 5 h. As Cr^{3+} ion content, x, increases from 0.02 to 0.10 (molar ratio of Cr/(Cr + Mn)), the average size varies slightly, which shows that the Cr content almost has no influence on the average size of the final products. On the other side, the lattice constant of $LiCr_xMn_{2-x}O$ spinel cell is decreased with Cr content (see Fig. 8). The radius of Cr^{3+} is 0.0615 nm, which is smaller than that of Mn^{3+} (0.0645 nm) [27], therefore, as Cr^{3+} ion content rises, the lattice parameter of the doped spinel decreases.

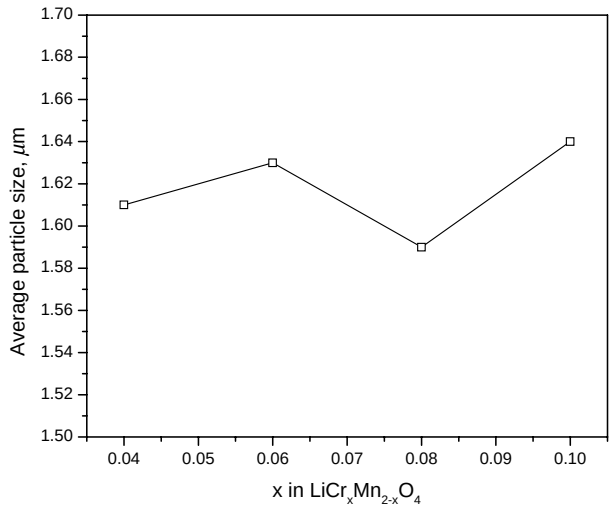

Fig. 7. Average particle size of $LiCr_xMn_{2-x}O_4$ synthesized at 650 °C for 2 h vs. Cr content.

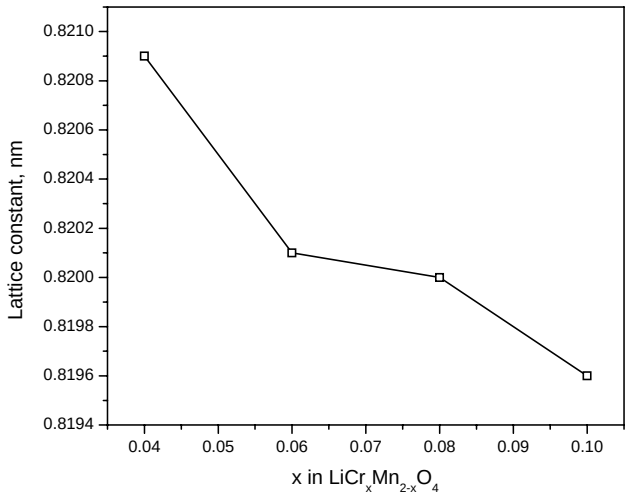

Fig. 8. Lattice constant as a function of Cr substitution of in $LiCr_xMn_{2-x}O_4$ synthesized at 650 °C.

3.3. Electrochemical behavior

The $Li/LiCr_{0.06}Mn_{1.94}O_4$ cell were electrochemically cycled 100 times. The cycle characteristics of products synthesized at 550–750 °C for 2 h are shown in Fig. 9. The product synthesized at 550 °C exhibited a lower discharge capacity compared with those products synthesized at 650 and 750 °C. The product synthesized at 650 °C delivered the highest initial charge capacity of 126 mAh/g and a corresponding discharge capacity of 120 mAh/g. The coulombic efficiency for the first cycle is 95%. The discharge capacity is well maintained at 104 mAh/g up to 100 cycles, showing a high reversible capacity and good cyclability. Usually the small particles with large interface area can provide more lithium ions for diffusion, thereby resulting in the high ionic current and specific capacity [33]. The mean particle size of the powders increased with increasing synthesis

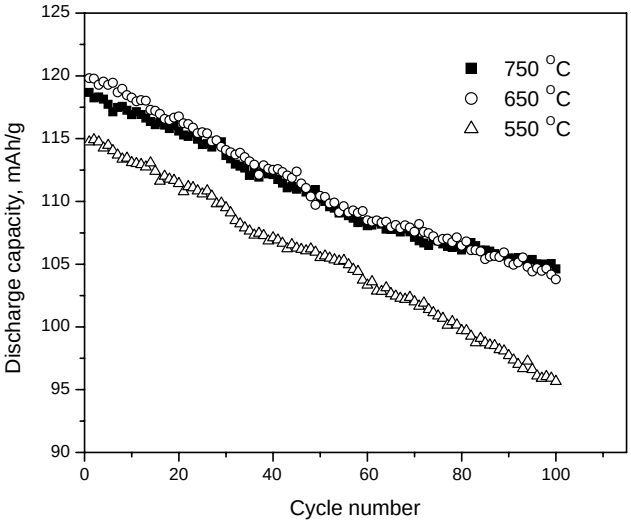

Fig. 9. Discharge capacity of $LiCr_{0.06}Mn_{1.94}O_4$ synthesized at various temperatures vs. cycle number.

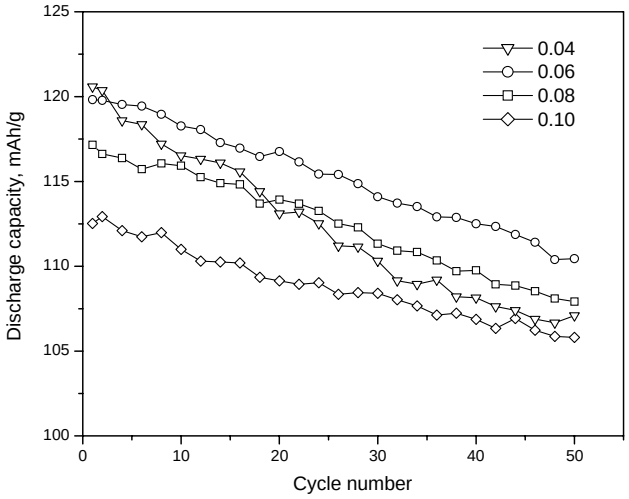

Fig. 10. Discharge capacity of Li/$LiCr_xMn_{2-x}O_4$ cell as a function of cycle number. $LiCr_xMn_{2-x}O_4$ ($0.04 \le x \le 0.10$) powders were synthesized at 650 °C.

temperature from 550 to 750 °C, as previously reported. So the sample synthesized at 550 °C should have the highest initial capacity. But the powders synthesized at 650 °C have the best electrochemical performance. The lower capacity of the powders synthesized at 550 °C is probably explained as that the lower synthesis temperature which did not deliver a very well-ordered Li–Mn–O spinel without any other impure phase (due to the limit resolution of XRD method), or may be due to the short calcining time, which is not enough for sufficient reaction to synthesize a high quality spinel.

Fig. 10 shows the relationship between the discharge capacity of the cathode and the cycle number for Li/$LiCr_xMn_{2-x}O_4$ cells. As expected, the doped spinels display good cycle performance in terms of discharge capacity and cycle-life. The good cyclability is probably due to the substitution of some Mn–O linkages in the spinel by Cr–O. The doped Cr^{3+} cations enhance the stability of the octahedral sites in the spinel skeleton structure [34]. The initial discharge capacities of these powders decrease with increasing Cr-substitution content in the active materials because of a decrease in the amount of extractable Li^+ ion in the spinel. For $LiCr_x$ $Mn_{2-x}O_4$, Cr^{3+} replaced the place occupied originally by Mn^{3+} and the amount of Mn^{3+} in spinel was reduced by the increasing amount of Cr^{3+}. Since Cr^{3+} ions cannot be oxidized in this potential range, the amount of removable Li^+ is determined by the amount of Mn^{3+} [35], and thus, only $(1-x)$ moles of Li^+ can be removed from per mole of $LiCr_xMn_{2-x}O_4$. During discharging, only a maximum of $(1-x)$ moles of Li can be re-inserted into each mole of cathode material, which is consistent with the results shown in Fig. 10. Inversely, as Cr content increases, the discharge capacity retention rate becomes better. The discharge capacity retention rate after 50 cycles is 89% for $LiCr_{0.04}Mn_{1.96}O_4$, 91% for $LiCr_{0.06}Mn_{1.94}O_4$, 92% for $LiCr_{0.08}Mn_{1.92}O_4$, and 94% for $LiCr_{0.10}Mn_{1.90}O_4$. The responding charge/discharge profiles of Li/$LiCr_xMn_{2-x}O_4$ cell for the 1st cycle and 50th cycle are shown in Fig. 11. The strength of Cr–O bonding is higher than Mn–O bonding on the basis of standard Gibbs energies of the formation of the both oxides at 298 K [36], thereby Cr cations enhance the stability of the octahedral sites in the spinel skeleton structure. As Cr content increases, the structure will become more stable, consequently, the initial capacity decreases and the cyclability increases, that is consistent with the results of Wang et al. [37] and Yoshio et al. [38] on Cr doped $LiMn_2O_4$. Considering the initial specific discharge capacity and the capacity retention rate, sample $LiCr_{0.06}Mn_{1.94}O_4$ exhibited good cycling performance, with initial discharge capacity of 120 mAh/g and capacity retention rate of 91% in this study. Zhang et al. [13] had reported that $LiCr_{0.1}Mn_{1.9}O_4$ showed best cycling performance among $LiCr_xMn_{2-x}O_4$ spinels ($x = 0$, 0.02, 0.05, 0.1) and its initial capacity increased with Cr content increased from 0.02 to 0.1, this tendency is some different from our present results and the results of Wang et al [37] and Yoshio et al. [38]. This different may be cause by the different preparation method and different Cr sources. Zhang et al. used a modified $mCrO_{2.66}$ instead of Cr_2O_3 and CrO_3 [13]. The effects of the amount of Cr substitution on the cycling performance and capacity are highly dependent on the thermal history and raw materials. The optimum Cr contents in spinel are basically between 0.05 and 0.1.

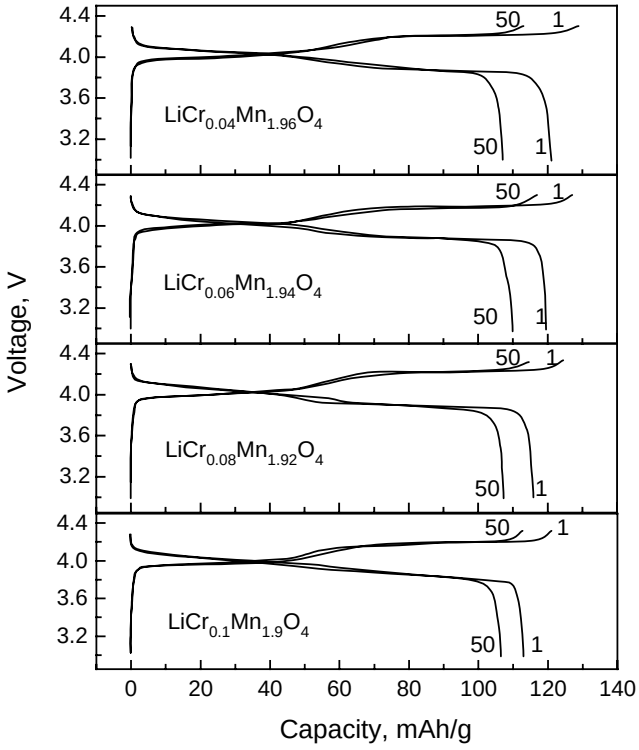

Fig. 11. Charge/discharge curves at the first cycle and 50th cycle of Li/$LiCr_xMn_{2-x}O_4$ cells, $LiCr_xMn_{2-x}O_4$ ($0.04 \le x \le 0.10$) powders were synthesized at 650 °C for 2 h.

The above results indicate that $LiCr_xMn_{2-x}O_4$ products with narrow particle size distribution and high capacity and

good cycle retention were successfully synthesized by a solid-state reaction at lower temperature for a shorter heating time. The rotary heating used in this study gives the prospect of continuously synthesizing oxide powders for Li-ion cathode materials with rotary furnaces. Once perfected, the mass production of cathode oxide powders by way of the high temperature rotary furnace should yield an excellent, consistent, reproducible, economical powder, possibly superior to many presently being produced.

4. Conclusions

In this paper, well-crystallized $LiCr_xMn_{2-x}O_4$ ($0.04 \leq x \leq 0.1$) spinels were prepared from the mixture of Li_2CO_3, Cr_2O_3 and MnO_2 using a technique of combining mechanical activation and rotary heating. The mechanically activated precursors of $LiCr_xMn_{2-x}O_4$ can be transferred into well-ordered spinels at lower heat treatment temperature for a shorter time. The rotary heating technology provided a homogeneous temperature field associated with stirring or tumbling action of the powders, which ensured that the final products have a good stability in structure, chemical composition and particle size distribution. The $LiCr_{0.06}Mn_{1.94}O_4$ powders synthesized at 650 °C for 2 h deliver high discharge capacities and good cycle retention. The technique of mechanical activation followed by rotary heating is easy, simple and cheap, and is ideally suited to the solid-state synthesis of lithium manganese oxides at lower temperature for a shorter time.

Acknowledgements

Financial support was provided by the China Postdoctoral Science Foundation and National Nature Science Foundation of China (No. 50101003). Appreciation is expressed to Ms. Hongqiong Peng for her helpful discussion on the electrochemical performance.

References

[1] R. Koksbang, J. Barker, H. Shi, M.Y. Saïdi, Solid State Ionics 84 (1996) 1.
[2] B. Scrosati, Electrochim. Acta 45 (2002) 2461.
[3] M. Salomon, B. Scrosati, Gazz. Chim. Ital. 126 (1996) 415.
[4] D. Song, H. Ikuta, T. Uchida, M. Wakihara, Solid State Ionics 117 (1999) 151.
[5] C. Julien, S. Ziolkiewicz, M. Lemal, M. Massot, J. Mater. Chem. 11 (2001) 1837.
[6] I.S. Jeong, J.U. Kim, H.B. Gu, J. Power Sources 102 (2001) 55.
[7] G. Kumar, H. Schlorb, D. Rahner, Mater. Chem. Phys. 70 (2001) 117.
[8] B. Banov, Y. Todorov, A. Trifonova, A. Momchilov, V. Manev, J. Power Sources 68 (1997) 578.
[9] K. Amine, H. Tukamoto, H. Yasuda, Y. Fujita, J. Power Sources 68 (1997) 604.
[10] Q. Feng, H. Hanoh, Y. Miyai, K. Ooi, Chem. Mater. 7 (1995) 379.
[11] G.B. Appetecchi, B. Scrosati, J. Electrochem. Soc. 144 (1997) L138.
[12] S.T. Myung, S. Komaba, N. Hirosaki, N. Kumagai, Electochem. Commun. 4 (2002) 397.
[13] D. Zhang, B.N. Popov, R.E. White, J. Power Sources 76 (1998) 81.
[14] P. Barboux, J.M. Tarascon, F.K. Shockoohi, J. Solid State Chem. 94 (1991) 185.
[15] V. Manev, A. Momchilov, A. Nassalevska, A. Kozawa, J. Power Sources 43–44 (1993) 551.
[16] G. Pistoia, G. Wang, C. Wang, Solid State Ionics 58 (1992) 285.
[17] J.M. Tarascon, E. Wang, F.K. Shokoohi, W.R. Mckinnon, S. Colson, J. Electrochem. Soc. 138 (1991) 2859.
[18] M. Yoshio, H. Noguchi, T. Miyashita, H. Nakamura, A. Kozawa, J. Power Sources 54 (1995) 483.
[19] Y. Xia, H. Takeshige, H. Noguchi, M Yoshio, J. Power Sources 56 (1995) 61.
[20] M. Morcrette, F. Gillot, L. Monconduit, J.M. Tarascon, Electrochem. Solid-State Lett. 6 (2003) A59.
[21] A. Rougier, S. Soiron, I. Haihal, L. Aymard, B. Taouk, J.M. Tarascon, Powder Technol. 128 (2002) 139.
[22] S. Soiron, A. Rougier, L. Aymard, J.M. Tarascon, J. Power Sources 97–98 (2001) 402.
[23] N.V. Kosova, I.P. Asanov, E.T. Devyatkina, E.G. Avvakumov, J. Solid State Chem. 146 (1999) 184.
[24] N.V. Kosova, E.T. Devyatkina, S.G. Kozlova, J. Power Sources 97–98 (2001) 406.
[25] N.V. Kosova, N.F. Uvarov, E.T. Devyatkina, E.G. Avvakumov, Solid State Ionics 135 (2000) 107.
[26] J.L. Tirado, Mater. Sci. Eng. R40 (2003) 103.
[27] R.D. Shannon, Acta Cryst. A32 (1976) 751.
[28] Y.M. Hon, H.Y. Chung, K.Z. Fung, M.H. Hon, J. Solid State Chem. 160 (2001) 368.
[29] R.J. Gummow, A. de Kock, M.M. Thackeray, Solid State Ionics 69 (1994) 59.
[30] A.R. Naghash, J.Y. Lee, J. Power Sources 85 (2000) 284.
[31] W. Liu, G.C. Farrington, F. Chaput, B. Dunn, J. Electrochem. Soc. 143 (1996) 879.
[32] Y.M. Hon, K.Z. Fung, M.H. Hon, J. Eur. Ceram. Soc. 21 (2001) 515.
[33] C.H. Lu, S.W. Lin, J. Power Sources 97–98 (2001) 458.
[34] K. Oikawa, T. Kamiyama, F. Izumi, D. Nakazato, H. Ikuta, M. Wakihara, J. Solid State Chem. 146 (1999) 322.
[35] M. Wohlfahrt-Mehrens, A. Butz, R. Oesten, G. Arnold, R.P. Hemmer, R.A. Huhhins, J. Power Sources 68 (1997) 582.
[36] D.R. Lide, Handbook of Chemistry and Physics, 76th ed., CRC Rress, London, 1995, pp. 5–72.
[37] G.X. Wang, D.H. Brandhurst, H.K. Liu, S.X. Dou, Solid State Ionics 120 (1999) 95.
[38] M. Yoshio, Y.Y. Xia, N. Kumada, S.H. Ma, J. Power Sources 101 (2001) 79.